Weed Science

www.cambridge.org/wsc

Target-site basis for fomesafen resistance in redroot pigweed (*Amaranthus retroflexus*) from China

Long Du[1,*], Xiao Li[1,*], Xiaojing Jiang[1], Qian Ju[1], Wenlei Guo[2], Lingxu Li[3], Chunjuan Qu[4] and Mingjing Qu[5]

[1]Research Assistant, Pest Bio-control Laboratory, Shandong Peanut Research Institute, Qingdao, China; [2]Research Assistant, Plant Protection Research Institute, Guangdong Academy of Agricultural Sciences, Guangdong Provincial Key Laboratory of High Technology for Plant Protection, Guangzhou, China; [3]Associate Professor, College of Plant Health and Medicine, Qingdao Agricultural University, Qingdao, China; [4]Associate Professor, Pest Bio-control Laboratory, Shandong Peanut Research Institute, Qingdao, China and [5]Professor, Pest Bio-control Laboratory, Shandong Peanut Research Institute, Qingdao, China

Research Article

Cite this article: Du L, Li X, Jiang X, Ju Q, Guo W, Li L, Qu C, Qu M (2021) Target-site basis for fomesafen resistance in redroot pigweed (*Amaranthus retroflexus*) from China. Weed Sci. **69**: 290–299. doi: 10.1017/wsc.2021.14

Received: 4 August 2020
Revised: 10 December 2020
Accepted: 9 February 2021
First published online: 22 February 2021

Associate Editor:
Mithila Jugulam, Kansas State University

Keywords:
Mutation; protoporphyrinogen oxidase (PPO); target-site resistance

Authors for correspondence:
Mingjing Qu, Shandong Peanut Research Institute, No. 126, Wannianquan Road, Qingdao, China.
Email: peanut205@163.com;
Chunjuan Qu, Shandong Peanut Research Institute, No. 126, Wannianquan Road, Qingdao, China.
Email: 2891240615@qq.com

*These authors contributed equally to this work.

Abstract

Redroot pigweed (*Amaranthus retroflexus* L.) is a dominant weed in soybean [*Glycine max* (L.) Merr.] fields in Heilongjiang Province, China. High selective pressure caused by the extensive application of the protoporphyrinogen oxidase (PPO)-inhibiting herbicide fomesafen has caused *A. retroflexus* to evolve resistance to this herbicide. Two susceptible and two resistant populations (S1, S2, R1, and R2) were selected in this study to illustrate the target-site resistance mechanism in resistant *A. retroflexus*. Whole-plant bioassays indicated that R1 and R2 had evolved high-level resistance to fomesafen, with resistance factors of 27.0 to 27.9. Sequence alignment of the *PPO* gene showed an Arg-128-Gly substitution in *PPX2*. The basal expression differences of *PPX1* and *PPX2* between the S1 and R1 plants were essentially nonsignificant, whereas the basal expression of *PPX2* in R2 plants was slightly lower than in S1 plants. Compared with the *PPX1* gene, the *PPX2* gene maintained higher expression in the resistant plants after treatment with fomesafen. An enzyme-linked immunosorbent assay showed a similar basal PPO content between the susceptible and resistant plants without treatment. After fomesafen treatment, the PPO content decreased sharply in the susceptible plants compared with the resistant plants. Furthermore, after 24 h of treatment, the resistant plants showed increased PPO content, whereas the susceptible plants had died. The *PPO2* mutation resulted in high extractable PPO activity and low sensitivity to fomesafen along with changes in PPO enzyme kinetics. Although the mutant *PPO2* exhibited increased K_m values in the resistant plants, the V_{max} values in these plants were also increased. Changes in the properties of the PPO enzyme due to an Arg-128-Gly substitution in *PPX2*, including changes in enzyme sensitivity and enzyme kinetics, are the target-site mechanism of resistance in *A. retroflexus*.

Introduction

Weed resistance to herbicides limits the number of effective herbicide options and has become a major obstacle to weed control worldwide. To date, weeds have evolved resistance to 23 of the 26 known active herbicide sites and 167 different herbicides (Heap 2020). The most common and strongest type of weed resistance is resistance to acetolactate synthase (ALS) inhibitors (HRAC Group B), followed by resistance to photosystem II (HRAC Group C1), 5-enolpyruvylshikimate-3-phosphate synthase (EPSPS) (HRAC Group G), and acetyl-CoA carboxylase (ACCase) inhibitors (HRAC Group A) (Heap 2020). Compared with weed resistance to the abovementioned types of herbicides, which are associated with a higher risk of resistance than other herbicides (Collavo et al. 2011; Tranel 2002), weed resistance to protoporphyrinogen oxidase (PPO) inhibitors seems to have evolved over a longer period of time. PPO-inhibiting herbicides have been used since the 1960s, but the first case of resistance to PPO inhibitors was reported in 2001 and involved waterhemp [*Amaranthus tuberculatus* (Moq.) Sauer] in soybean [*Glycine max* (L.) Merr.] fields (Dayan et al. 2014; Shoup et al. 2003). Since then, resistance to PPO inhibitors has evolved in wild poinsettia (*Euphorbia heterophylla* L.), common ragweed (*Ambrosia artemisiifolia* L.), Palmer amaranth (*Amaranthus palmeri* S. Watson), and redroot pigweed (*Amaranthus retroflexus* L.) (Rousonelos et al. 2012; Salas et al. 2016; Trezzi et al. 2005; Wang et al. 2017). The widespread cultivation of glyphosate-resistant soybean has reduced dependence on PPO-inhibiting herbicides, which has reduced the selection pressure for resistance to PPO inhibitors (Young 2006). However, in the past two decades, growers' dependence on PPO-inhibiting herbicides has increased as weeds have developed resistance to glyphosate

and ALS inhibitors (Chen et al. 2015; Legleiter et al. 2009; Salas et al. 2016). Consequently, resistance to PPO inhibitors has evolved over the past two decades.

Plant PPO catalyzes the conversion of protoporphyrinogen IX to protoporphyrin IX in the tetrapyrrole biosynthethic pathway, which produces heme and chlorophyll (Deybach et al. 1985; Poulson and Polglase 1975). There are two isoforms of PPO, plastid-targeted and mitochondrial-targeted PPO (namely, PPO1 and PPO2), which are encoded by the *PPX1* and *PPX2* genes, respectively (Lermontova et al. 1997). In some plant species, PPO2 is dual-targeted in plastids and mitochondria (Watanabe et al. 2001). PPO-inhibiting herbicides reduce the conversion of protoporphyrinogen IX to protoporphyrin IX, and the accumulated protoporphyrinogen IX is transported to the cytoplasm and spontaneously undergoes peroxidation to form protoporphyrin IX. Under light conditions, the accumulated protoporphyrin IX produces singlet oxygen, which can cause lipid membrane oxidation and plant injury (Jacobs and Jacobs 1993; Jacobs et al. 1991; Lee and Duke 1994). These two isoforms of PPO are the targets of PPO-inhibiting herbicides.

To date, a total of 13 species of weeds have developed resistance to PPO-inhibiting herbicides (Heap 2020). In most of the reported cases of field-evolved resistance, resistance is caused by target-based mutations. Five amino acid mutations in *PPX2* located at three sites have been reported to cause herbicide resistance to PPO-inhibiting herbicides in weeds. One mutation is a deletion of glycine at position 210 (Gly-210) in *PPX2* (Lee et al. 2008; Patzoldt et al. 2006; Salas et al. 2016). This position serves an important stabilizing role in the capped region of the α-8 helix, and its absence unwinds the last turn of the helix, thus causing the cavity of the active site to expand by approximately 50%; this expansion reduces the binding of herbicides and PPO (Dayan et al. 2010; Yang et al. 2013). Another mutation is an amino acid substitution of arginine at position 128 (or 98), present as Arg-98-Leu in *A. artemisiifolia*, Arg-128-Gly and Arg-128-Met in *A. palmeri*, Arg-128-Gly in *A. retroflexus*, and Arg-128-Ile and Arg-128-Lys in *A. tuberculatus* (Giacomini et al. 2017; Huang et al. 2020; Nie et al. 2019; Varanasi et al. 2018b). The Arg-128 and Arg-98 positions are homologous, and the difference in the code number results because there is a 30-amino-acid signal peptide in *A. palmeri* but not in *A. artemisiifolia*. Position 128 is highly conserved among multiple plant species, and this site plays an important role in substrate positioning. Therefore, an amino acid substitution at this site is generally associated with herbicide resistance (Dayan et al. 2018; Nie et al. 2019). Recently, a novel substitution of glycine with alanine at position 399 (Gly-399-Ala), which is located in the catalytic domain of PPO, was reported in *A. palmeri* (Rangani et al. 2019). The steric hindrance caused by Gly-399-Ala results in a reduced affinity for PPO-inhibiting herbicides (Rangani et al. 2019). In addition, although non–target site based resistance to this class of herbicides has been reported in only a few cases, involving species such as *A. tuberculatus* and *A. palmeri*, it cannot be ignored (Obenland et al. 2017; Varanasi et al. 2018a, 2019).

Amaranthus retroflexus occurs in autumn crops, such as soybean, cotton (*Gossypium hirsutum* L.), peanuts (*Arachis hypogaea* L.), and corn (*Zea mays* L.), in fields in most areas of China. Additionally, it is one of the dominant weeds in soybean fields in Heilongjiang Province. In the past few years, with the evolution of resistance to ALS-inhibiting herbicides, PPO-inhibiting herbicides, especially fomesafen, have become the main herbicides for controlling this weed (Chen et al. 2015). Under the selective pressure of PPO-inhibiting herbicides, *A. retroflexus* has evolved resistance to fomesafen (Wang et al. 2017). Several studies have indicated that the Arg-128-Gly mutation in *PPO2* is one of the target site–based resistance mechanisms in *A. retroflexus*, but more comprehensive and detailed information has thus far not been discovered (Huang et al. 2020; Wang et al. 2019). Therefore, the objectives of this study were to characterize the fomesafen sensitivity of susceptible and resistant *A. retroflexus* and to systematically illustrate the target site–based resistance mechanism, including variations in the *PPO* gene sequence, PPO enzyme activity, enzyme kinetics, and PPO expression.

Materials and Methods

Plant Material

Fifty-six suspected resistant *A. retroflexus* populations were collected from areas where fomesafen control failed. The sampling area included approximately 7,000 km^2 in Heilongjiang Province, China. The central coordinates of the collection area are approximately 125.26°N and 49.18°E. Two susceptible populations (referred to as S1 and S2) were collected from noncultivated land areas (124.03°N, 47.36°E) with a geographic distance of approximately 200 km from where resistance evolved. Approximately 10 plants were collected from each population, and then the seeds were air-dried and stored in paper bags at room temperature until use.

Whole-Plant Bioassay

Seeds were germinated for 5 d in 9-cm-diameter petri dishes containing two layers of filter paper and 5 ml of deionized water at 25 C. Seedlings were transplanted to plastic pots (5 seedlings per pot) containing a commercial nutrient matrix and grown in phytotrons set at 25 C/16-h day, 18 C/8-h night, 65% relative humidity, and a light intensity of 12,000 lx. A single-dose bioassay with 250 g ai ha^{-1} fomesafen was conducted first to screen the resistant populations, with the S1 and S2 populations serving as susceptible controls. After that, two resistant populations (referred to as R1 and R2) approximately 50 km apart were selected to determine their sensitivity to fomesafen with S1 and S2 as controls. In addition, all plants from both resistant populations survived a dose of 250 g ai ha^{-1}. The treatment doses of fomesafen were 0, 0.514, 1.54, 4.63, 13.89, 41.67, and 125 g ai ha^{-1} (0-, 1/729-, 1/243-, 1/81-, 1/27-, 1/9- and 1/3-fold the recommended dose, respectively) for the susceptible populations and 0, 4.63, 13.89, 41.67, 125, 375, and 1,125 g ai ha^{-1} (0-, 1/81-, 1/27-, 1/9-, 1/3-, 1-, and 3-fold the recommended dose, respectively) for the resistant populations. All tested populations were directly cultivated with seeds collected in the field. Seedlings were treated with fomesafen once they reached a 10-cm height using an automatic spraying system equipped with a TeeJet® 9503EVS flat-fan spray nozzle (Spraying Systems, Wheaton, IL, USA). The spray volume was 300 L ha^{-1} at 0.28 MPa. The aboveground biomass of each treatment was collected after 3 wk of treatment and dried at 70 C for 72 h, and then the dry weights were recorded. Each treatment consisted of four replicates, and the entire experiment was repeated twice.

PPO Gene Amplification and Sequencing

Total RNA was extracted from 10 individual plants within each resistant and susceptible population using an EasyPure Plant

https://doi.org/10.1017/wsc.2021.14 Published online by Cambridge University Press

Table 1. Primers used in this study.

Primers	Sequence (5′→3′)	Temperature used in PCR C	Purpose of primers
PPX1-F	CTCCGACATCTCGTTCC	58	Amplify nearly full-length *PPX1*
PPX1-R	ACCCTCTATACACCTCCC		
PPX2-F	TCCATTACCCACCTTTCACC	58	Amplify nearly full-length *PPX2*
PPX2-R	TTACGCGGTCTTCTCATCCAT		
PPX1-qF	CCTAATAGTTTCCAACCCTCC	59	qRT-PCR assay for *PPX1*
PPX1-qR	TTACCATTCCAGAGCACGA		
PPX2-qF	ATGACAGAAAGTGAGGCAGAG	59	qRT-PCR assay for *PPX2*
PPX2-qR	AAGGTAGTAGCACCGGAAG		
Actin-qF	TGCTGGTCGTGATCTTACTG	59	qRT-PCR assay for *actin*
Actin-qR	CCTCTGGGCAACGGAAT		

RNA kit (TransGen Biotech, Beijing, China). Then, cDNA was synthesized using Transcript a First Strand cDNA Synthesis Kit with DNA removal (TransGen Biotech). Two nearly full-length *PPX1* and *PPX2* genes were amplified with the primers PPX1F/PPX1R and PPX2F/PPX2R (Table 1). The primers for amplifying nearly full-length *PPX1* were designed by Primer Premier 5.0 (PREMIER Biosoft, San Francisco, CA, USA) according to the *PPX1* sequence of *A. tuberculatus* (GenBank accession no. DQ386112) and synthesized by a commercial sequencing company (Personal Biotech, Shanghai, China). The primers for amplifying *PPX2* were synthesized according to a previous study (Giacomini et al. 2017). PCR was conducted in a 25-µl volume that consisted of 1 µl of cDNA (60 ng), 1 µl of each primer (1 µM), and 22 µl of Taq Master Mix (US Everbright, Suzhou, China). PCR for amplifying *PPX1* and *PPX2* was performed on a thermal cycler (Bio-Rad, Hercules, CA, USA) with the following profile: 94 C for 5 min; 33 cycles at 94 C for 30 s, 58 C for 30 s, and 72 C for 80 s; and a final extension at 72 C for 5 min. The PCR products were sequenced by Personal Biotech. Sequence alignment was conducted using DNAMAN 9.0 (Lynnon Biosoft, San Ramon, CA, USA), and amino acid numbering for *PPX1* and *PPX2* was performed based on that of *A. tuberculatus* (GenBank accession nos. DQ386112, DQ386114).

In Vitro PPO Assay

The PPO activity assay was conducted by measuring the formation rate of protoporphyrin IX at 30 C according to the fluorometric method (Ishida et al. 2000; Nicolaus et al. 1993). Seedling preparation was conducted as described earlier. The leaves (1 g) were harvested after exposure to light for 12 h and homogenized in 5 ml of an extraction buffer with a pH of 7.3 containing 0.05 M HEPES buffer, 0.5 M sucrose, 1 mM 1,4-dithiothreitol (DTT), 1 mM $MgCl_2$, 1 mM ethylenediaminetetraacetic acid (EDTA), and 0.2% bovine serum albumin (BSA). After two steps of centrifugation (800 × *g* for 2 min and then 17,000 × *g* for 6 min), the precipitate was dissolved again in a lysosomal buffer with a pH of 7.3 containing 0.05 M Tris and 2 mM EDTA. PPO inhibition was determined after adding 100 µl of fomesafen (0 to 100 µM) to a final assay volume of 3 ml of reaction buffer containing 0.1 mM Tris, 1 mM EDTA, 5 mM DTT, 1% (v/v) Tween-80, 100 µl of crude PPO, and approximately 8 µM protoporphyrinogen IX. The reaction system was placed in a 30 C water bath and shaken in the dark for 30 min. The protoporphyrinogen IX was freshly obtained by reducing protoporphyrin in the dark with a sodium amalgam in a nitrogen atmosphere. The protein content of the crude extraction enzyme was measured using the Bradford method (Bradford 1976). The amount of protoporphyrin produced was measured with a Hitachi F-2700 fluorescence spectrophotometer (Hitachi, Tokyo, Japan) using an excitation wavelength of 405 nm and an emission wavelength of 633 nm (Rangani et al. 2019). The PPO activity was calculated by the amount of protoporphyrin produced per unit of time (nmol Proto-IX mg protein^{-1} h^{-1}). For the PPO enzyme kinetic assay, protoporphyrinogen IX was omitted from the reaction mixture, and serial protoporphyrinogen IX concentrations of 0.5, 1, 2, 3, 4, 5, 7, 9, and 10 µM were used in the final reaction system. There were three technical replicates for each sample and three biological replicates for each treatment. The entire experiment was repeated two times.

PPO Expression Assay

A PPO expression assay was conducted at the transcription and translation levels. *Amaranthus retroflexus* seedlings were prepared as described earlier and treated with fomesafen at a dose of 37.5 g ai ha^{-1} after growing to a height of 10 cm. The foliage of the resistant and susceptible populations was harvested at 0 (untreated control), 6, 12, 24, and 48 h after treatment (HAT). Total RNA extraction and cDNA synthesis were conducted as described earlier.

PPO gene expression, including *PPX1* and *PPX2*, was determined by real-time quantitative reverse transcriptase PCR (qRT-PCR) in an AB 7500 Fast Real-Time PCR system (Applied Biosystems, Dun Laoghaire, County Dublin, Ireland) using TB Green Fast qPCR Mix (Takara, Dalian, China). The *actin* gene was selected as the internal reference gene (Huang et al. 2016). The primers used in the qRT-PCR assay were PPX1-qF/PPX1-qR, PPX2-qF/PPX2-qR, and actin-qF/actin-qR (Table 1). The primers were designed by Primer Premier 5.0, and the primers used for amplifying *actin* were designed according to the *actin* sequence of silver cock's comb (*Celosia argentea* L.) (GenBank accession no. HQ844002.1). To determine the specificity and amplification efficiency of primers, melting and standard curves were generated. A three-step profile was used in thermal cycling: 94 C for 5 s, 59 C for 30 s, and 72 C for 5 s. The Ct values of each sample were recorded, and the relative expression levels of *PPX1* and *PPX2* were calculated with the $2^{-\Delta\Delta Ct}$ method ($\Delta Ct = Ct_{ppx} - Ct_{Actin}$, $\Delta\Delta Ct = \Delta Ct_{treated} - \Delta Ct_{untreated}$). The *actin* gene served as the endogenous control, and the untreated sample served as the reference sample. Each sample was set up with three technical repeats and two biological repeats. The entire experiment was repeated two times.

The determination of the PPO enzyme content was carried out using an enzyme-linked immunosorbent assay (ELISA) kit (Jianglai Bio, Shanghai, China). The kit was only used to determine the PPO content without distinguishing between plastid PPO and mitochondrial PPO, not to measure PPO activity. Foliage material (0.5 g) from each harvested plant material sample was

https://doi.org/10.1017/wsc.2021.14 Published online by Cambridge University Press

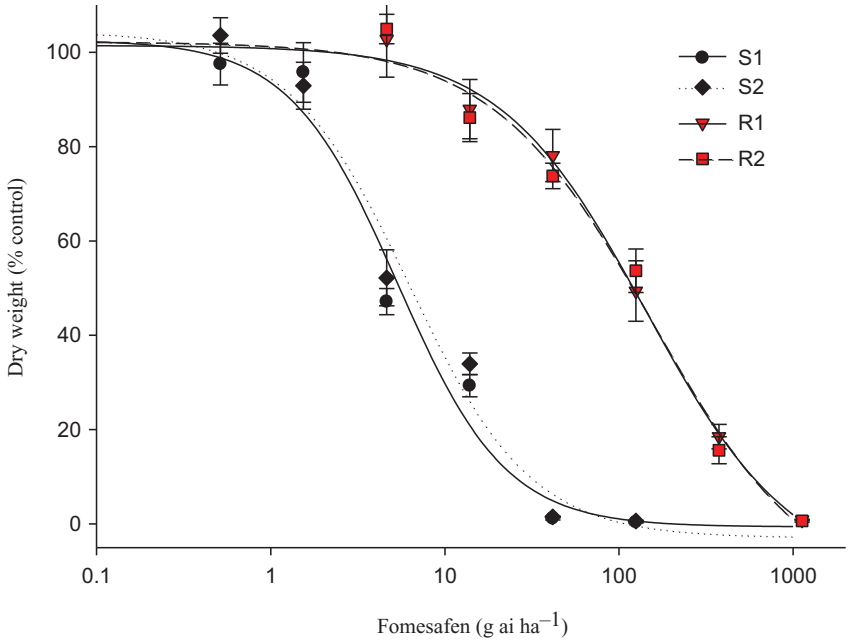

Figure 1. Dose–response curve fit to a four-parameter nonlinear regression model for aboveground dry weights of the *Amaranthus retroflexus* populations treated with fomesafen. Mean values and their SEs are shown.

homogenized in 5 ml of extraction buffer at 0 C. Subsequent procedures were carried out following the instructions in the product manual. A standard curve was made according to the standard products provided by the ELISA kit, and then the PPO content was calculated according to the standard curve obtained. Each sample was set up with three technical repeats and three biological repeats. The entire experiment was repeated two times.

Statistical Analysis

The dose–response data (including plant growth and enzyme activity inhibition) were analyzed by ANOVA using SPSS v. 20.0 (IBM SPSS, Chicago, IL, USA). The data were pooled if there was no significant difference between two experimental trials. Means were analyzed using Fisher's protected LSD test at the 5% level of probability. Dose–response data were fit to the four-parameter logistic equation (Equation 1) proposed by Seefeld et al. (1995) using SigmaPlot v. 12.5 (Systat, San Jose, CA, USA) to calculate the GR_{50} (or I_{50}).

$$y = C + \frac{D - C}{1 + \left(\frac{x}{GR_{50}}\right)^{b}} \quad [1]$$

where x represents the herbicide concentration, y represents % of control, C represents the lower limit, D represents the upper limit and GR_{50} (or I_{50}) represents the herbicide dose causing 50% growth inhibition (or enzyme activity).

For enzyme kinetics, the K_m values were calculated by fitting the data to the Michaelis-Menten equation (Equation 2) using SigmaPlot 12.5 (Systat).

$$v = \frac{V_{max} S}{K_m + S} \quad [2]$$

where v represents the catalytic velocity, S represents the substrate concentration and V_{max} represents the maximum catalytic velocity.

Results and Discussion

Whole-Plant Bioassay

The dose–response experiments at the whole-plant level indicated that the two resistant populations showed significantly different responses to fomesafen than did the two susceptible populations. Fomesafen (recommended dose 375 g ai ha^{-1}) at a dose of 41.7 g ai ha^{-1} caused clear evidence of injury in the susceptible plants within 2 d after treatment (DAT), and these plants died within 7 DAT. Fomesafen did not kill the susceptible plants at doses below 13.9 g ai ha^{-1}, but their growth was severely inhibited as the dose increased from 4.6 to 13.9 g ai ha^{-1}, with chlorosis, stunting, and crinkling leaves providing evidence of injury. However, fomesafen at doses from 4.6 to 13.9 g ha^{-1} had little effect on the growth of resistant plants, which exhibited no evidence of injury such as chlorosis or stunting. All plants from both the R1 and R2 populations survived the recommended dose of 375 g ha^{-1} (Figure 1). Although the growth of the resistant plants was significantly inhibited, it should be noted that this result was obtained under phytotron conditions, which usually causes weeds to be more sensitive to herbicides than under natural conditions. The high resistance factors (27.0 and 27.9) of the R1 and R2 populations indicated a high level of resistance to fomesafen. At doses of 41.7 and 125 g ha^{-1}, the resistant plant foliage was injured, but the growing point and damaged leaves recovered and resumed growth at 10 DAT. The average GR_{50} value for the two susceptible populations was 5.77 g ha^{-1} (5.35 for S1 and 6.18 for S2, respectively). The GR_{50} values for the two resistant populations (R1 and R2) were 143.6 and 155.7 g ha^{-1}, respectively, and the calculated resistance factors were 27.9 and 27.0, respectively (Table 2).

We investigated the resistance of *A. retroflexus* in an area of 7,000 km^2 in Nenjiang County, Heilongjiang Province. The results showed that almost all populations developed the same resistance as observed in the R1 and R2 populations tested in this study (data not shown). In practice, some growers use a 5-fold dose of

https://doi.org/10.1017/wsc.2021.14 Published online by Cambridge University Press

Table 2. Parameter estimates from the logistic analysis of growth inhibition by fomesafen for the susceptible and resistant *Amaranthus retroflexus* populations.[a]

Population	*C*	*D*	*b*	GR_{50}	Rf[b]
S1	−0.608 ± 0.089	102.6 ± 7.5	−1.40 ± 0.5	5.35 ± 1.51	—
S2	−2.84 ± 0.97	104.5 ± 7.1	−1.21 ± 0.4	6.18 ± 1.79	—
R1	−11.38 ± 9.4	101.4 ± 3.0	−1.03 ± 0.2	143.6 ± 31.6	27.9
R2	−16.56 ± 19.15	102.2 ± 5.4	−0.95 ± 0.28	155.7 ± 68.5	27.0

[a]*C*, lower limit; *D*, upper limit; *b*, the slope at GR_{50}; Rf, resistance factor.
[b]Rf values were calculated as the mean values of the two susceptible populations. Fitting parameters and their SEs are shown.

fomesafen to improve the control efficacy of *A. retroflexus*. The poor fomesafen efficacy against *A. retroflexus* indicated the evolution of herbicide resistance, which could be attributed to the pervasive practice of soybean monoculture in this area along with the repeated use of fomesafen over a 30-yr period (Huang et al. 2020; Wang et al. 2019). Herbicides with specific targets nearly always seem to induce resistance in plants after years of continuous application. In addition, *A. retroflexus* in this area has evolved high resistance to ALS inhibitors in the past few years, and thus, the overreliance on PPO-inhibiting herbicides in this area has provided greater selection pressure for PPO-inhibitor resistance (Chen et al. 2015; Huang et al. 2016; Wang et al. 2017, 2019).

PPX1 and PPX2 Gene Amplification and Sequencing

Two nearly full-length *PPX1* and *PPX2* transcripts of 10 individual plants from each population (R1, R2, S1, and S2) were obtained by amplifying cDNA with the two pairs of primers PPX1-F/PPX1-R and PPX2-F/PPX2-R (Table 1). The lengths of the two amplified genes were 1,529 bp and 1,549 bp, respectively. Three known point mutations endowing herbicide resistance were encompassed in the *PPX2* transcripts, including Gly-210, Arg-128, and Gly-399. Sequence alignment in *PPX1* revealed that one homozygous codon changed from GCA to GGA at site 292 in all tested resistant plants, which led to an amino acid change from Gly to Ala. However, this codon change did not seem to provide herbicide resistance, because the Ala-292 codon was detected in the susceptible *A. tuberculatus* plants (GenBank accession no. DQ386112). All amplified *PPX2* transcripts from the resistant plants included a substitution of the AGG codon at site 128 with GGG, which resulted in an amino acid change from Arg to Gly. The sequencing chromatograms indicated that all Arg-128-Gly mutations were homozygous in the 10 resistant plants of each resistant population (Supplemental Figure). No other single-nucleotide polymorphisms were found in the tested plants.

Target gene mutations endowing weed resistance to herbicides are prevalent in agricultural production (Powles and Yu 2010). A crystal structure assay of PPO indicated that Arg-128 was highly conserved and was located at a substrate-binding site (Heinemann et al. 2007; Koch et al. 2004). Therefore, alterations at this site may result in changes in functional proteins. To date, it has been clarified that four types of Arg-128 substitutions in *PPX2* can cause weed resistance to herbicides, including Arg-128-Gly in *A. palmeri* and *A. retroflexus*, Arg-128-Met in *A. palmeri*, Arg-128-Ile in *A. tuberculatus*, and Arg-128-Leu in *A. artemisiifolia* (Giacomini et al. 2017; Nie et al. 2019; Rousonelos et al. 2012; Wang et al. 2019). In this study, two resistant populations containing the Arg-128-Gly mutation showed highs level of resistance to fomesafen with resistance ratios of 27.0 to 27.9. Generally, the *PPO* Arg-128-Gly mutation confers upon weeds high levels of resistance (resistance ratio >10) to diphenyl ethers (e.g., fomesafen, lactofen, fluoroglycofen-ethyl, and acifluorfen). The published literature indicated that the greatest level of resistance to diphenyl ether herbicides was with fomesafen, with resistance levels of 80.2-fold in *A. artemisiifolia* and 41.8-fold in *A. retroflexus* (Rousonelos et al. 2012; Wang et al. 2019). However, not all Arg-128 substitutions endow weed resistance to herbicides; for example, Arg-128-Lys retains sensitivity to fomesafen because of a similarly sized and positively charged side chain (Nie et al. 2019). In addition, two types of artificially altered Arg-128 can occur after changing one nucleotide, with Arg-128-Ser and Arg-128-Thr endowing fomesafen resistance (Nie et al. 2019). However, neither mutation has yet been found in the field.

In plants, there are two types of PPO, plastid-targeted PPO (PPO1) encoded by the *PPX1* gene and mitochondria-targeted PPO (PPO2) encoded by the *PPX2* gene (Lermontova et al. 1997), and both types of PPO are targets of PPO inhibitors. Consistent with all previous reports of weeds resistant to PPO inhibitors, no mutations suspected of endowing resistance were identified in the *PPX1* gene of the 20 plants from the two resistant populations. Therefore, PPO2 played a more important role in the evolution of PPO-inhibitor resistance. One plausible explanation is the distribution of PPO2 in organelles (Dayan et al. 2014). In *Amaranthus* species, *PPX2* encodes dual-targeted PPO2 due to a signaling sequence for plastid import (Emanuelesson et al. 2000; Patzoldt et al. 2006). Therefore, PPO activity in both plastids and mitochondria will be protected when the mutation endowing resistance occurs in PPO2 in the presence of PPO inhibitors. If the resistance mutation is present in PPO1, the susceptible mitochondria-targeted PPO is still inhibited by PPO inhibitors, and thus the plants are still sensitive to PPO inhibitors.

PPO Expression Assay by qRT-PCR and ELISA

In this study, the expression level of PPO was explored at the transcription level and translation level by qRT-PCR and ELISA, respectively. To verify the specificity and amplification efficiency of primers used for qRT-PCR, the melting and standard curves were obtained. The results showed that the melting curves were all single peaks with melting temperatures >82 C and amplification efficiencies of 102.3% to 106.8%. A commercial ELISA kit for the determination of the PPO content was used in this experiment.

Twenty-three pots (with 5 plants per pot) of each population were treated with fomesafen at a dose of 37.5 g ha^{-1}, which is higher than the GR_{50} value of S1 plants. Fomesafen at this rate caused susceptible plants to stunt within 6 h and undergo necrosis within 24 HAT. The quality of RNA extracted from the S1 plant leaves sampled at 24 HAT was too low to perform qRT-PCR. Therefore, the *PPO* gene expression of S1 plants 24 HAT is not shown in the results. During the observation time, the *PPX1* and *PPX2* genes were affected by fomesafen and exhibited reduced

https://doi.org/10.1017/wsc.2021.14 Published online by Cambridge University Press

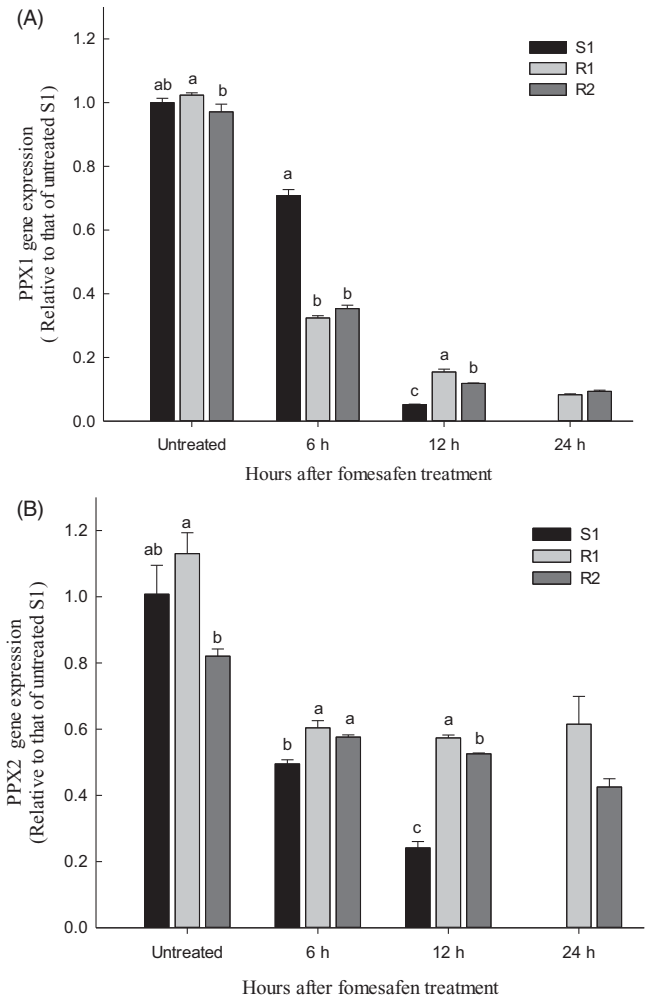

Figure 2. Gene expression levels of *PPX1* (A) and *PPX2* (B) over time in the susceptible and resistant plants after treatment with fomesafen. The gene expression level was calculated with the $2^{-\Delta\Delta}$ method. The *actin* gene served as an internal reference gene for normalizing the variations in cDNA amounts, and the untreated susceptible populations served as a control. Mean values and their SEs are shown. Different lowercase letters indicate significant differences at the 5% level as determined by the LSD test within treatment times.

expression in both the susceptible and resistant plants over time (Figure 2). However, the degree of reduction is different. *PPX1* gene expression was severely suppressed, with reductions of approximately 90% in the resistant plants at 24 HAT and more than 90% in the susceptible plants at 12 HAT. Compared with the *PPX1* gene expression, the *PPX2* gene expression was less affected by fomesafen, especially in the resistant plants. The variation trends of the *PPX1* and *PPX2* gene expression in the two resistant populations were the same (Figure 2). No significant difference in basal *PPO* gene expression was observed between the susceptible and resistant populations (Figure 2). The expression level of the *PPX1* gene in S1 plants was higher than that of the resistant plants after 6 h of treatment, but after 12 h, the *PPX1* expression level quickly decreased to a level significantly lower than that of the resistant plants (Figure 2A). The expression of the *PPX2* gene in the S1 plants continuously decreased over time, dropping from 0.55 to 0.13 (relative to the expression of the internal reference gene) within 12 HAT, whereas the expression of the *PPX2* gene in the resistant plants remained at approximately 0.3 (relative to the expression of the internal reference gene). At 24 HAT, the expression of the *PPX2* gene in resistant plants had not changed significantly from that at 6 or 12 HAT (Figure 2B).

ELISA revealed a similar basal PPO content between the susceptible and resistant plants without fomesafen treatment (Figure 3). After fomesafen treatment, the content of PPO continuously decreased within 24 HAT, from 36.4 to 15.5 ng/g in the R1 plants and from 37.9 to 18.3 ng/g in the R2 plants, before slowly increasing. However, the PPO content of S1 plants decreased over time in association with the intensification of injury symptoms and was no longer detectable at 24 HAT. In the R1 and R2 plants, the trend of the PPO content was the same (Figure 3).

Overexpression of the target enzyme is another mechanism of weed target-site resistance, including gene amplification and changes in the gene promoter (Odell et al. 1990; Powles 2010). The most common case is glyphosate resistance caused by *EPSPS* gene amplification (Gaines et al. 2010). The expression level of PPO in the resistant and susceptible plants was the same at transcription and translation levels without the fomesafen treatment (Figures 2 and 3). After fomesafen treatment, both the PPO enzyme protein and *PPO* gene expression (*PPX1* and *PPX2*) significantly decreased within 24 h, but the resistant plants showed weaker decreases than the susceptible plants, especially with respect to *PPX2* gene expression and enzyme protein content (Figures 2 and 3). Although the PPO transcription and content of the resistant plants were significantly suppressed, the plants were free of significant visual damage and grew normally. After 48 h of fomesafen treatment, a slight increase in the PPO enzyme content indicated that resistant plants would gradually return to normal growth without being affected by the agent (Figure 3). It should be noted that the *PPX1* and *PPX2* genes seem to play different roles in herbicide resistance. In resistant plants, the expression of *PPX1* may be suppressed due to an unknown feedback regulation mechanism (Hao et al. 2013), but *PPX2* is maintained at a high level relative to *PPX1*. We suspect that *PPX2* is less susceptible to some type of feedback regulation because of the dual-targeted peculiarity of PPO2. In this regard, *PPX2* seems to play a more important role in herbicide resistance than *PPX1*.

In Vitro Assay of PPO Activity

In vitro assays indicated that the basal PPO activity of resistant plants was significantly higher than that of susceptible plants (Figure 4). In the absence of fomesafen, the extractable PPO activity was 3.42 nmol Proto-IX mg protein^{-1} h^{-1} in the S1 plants, and 5.45 and 5.58 nmol Proto-IX mg protein^{-1} h^{-1} in the R1 and R2 plants, respectively (Figure 4). Due to the similar expression levels of PPO between the resistant and susceptible plants without fomesafen treatment, it can be concluded that the increase in extractable PPO activity in resistant plants was not related to the expression of PPO but was related to the Arg-128-Gly mutation, which might contribute to fomesafen resistance. The results of the fomesafen sensitivity analysis of PPO are shown in Table 3 and Figure 5. A wild-type PPO isolated from the S1 plants was observably inhibited by fomesafen, with an I_{50} value of 0.091 μM (Table 3; Figure 5). However, PPO isolated from the R1 and R2 plants was significantly less inhibited by fomesafen than was wild-type PPO, with I_{50} values of 11.36 and 19.32 μM, respectively (Table 3; Figure 5). The fomesafen I_{50} values for R1 and R2 were 124.7- and 212.3-fold greater than those of the S1 plants, respectively (Table 3). Thus, as expected, the Arg-128-Gly mutation resulted in insensitive PPO,

https://doi.org/10.1017/wsc.2021.14 Published online by Cambridge University Press

Table 3. Parameter estimates from the logistic analysis of in vitro inhibition of PPO activity by fomesafen for the susceptible and resistant *Amaranthus retroflexus* populations.[a]

Population	*C*	*D*	*b*	I_{50} µM	R/S ratio
S1	9.4 ± 4.0	88.3 ± 6.2	−0.9 ± 0.3	0.091 ± 0.03	
R1	−6.2 ± 1.7	97.3 ± 3.1	−0.7 ± 0.2	11.36 ± 6.75	124.7
R2	−27.8 ± 17.9	101.3 ± 1.8	−0.5 ± 0.07	19.32 ± 11.54	212.3

[a]*C*, lower limit; *D*, upper limit; *b*, the slope at I_{50}. Fitting parameters and their SEs are shown.

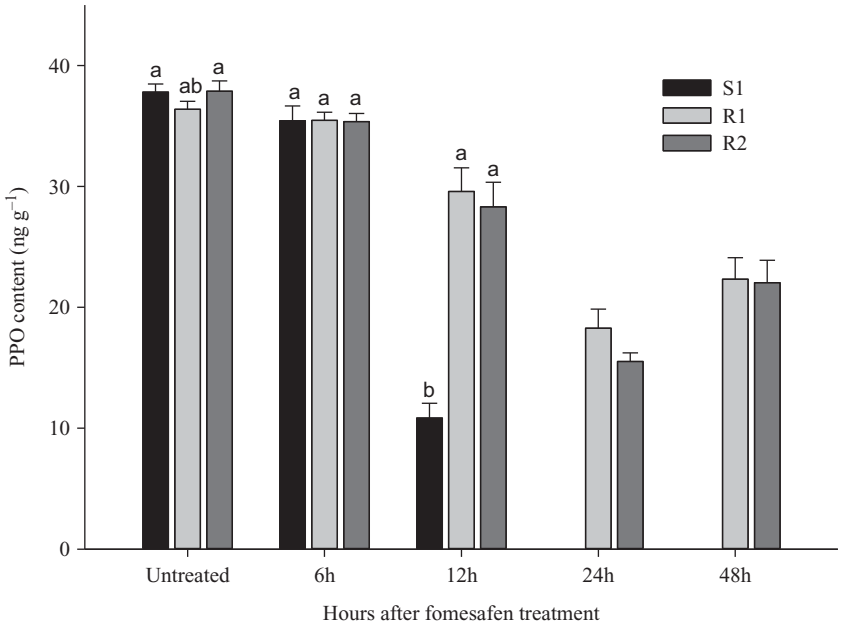

Figure 3. Basal and induced PPO content variation in the susceptible and resistant plants after the fomesafen treatment using an enzyme-linked immunosorbent assay. Mean values and their SEs are shown. Different lowercase letters indicate significant differences at the 5% level as determined by the LSD test within treatment times.

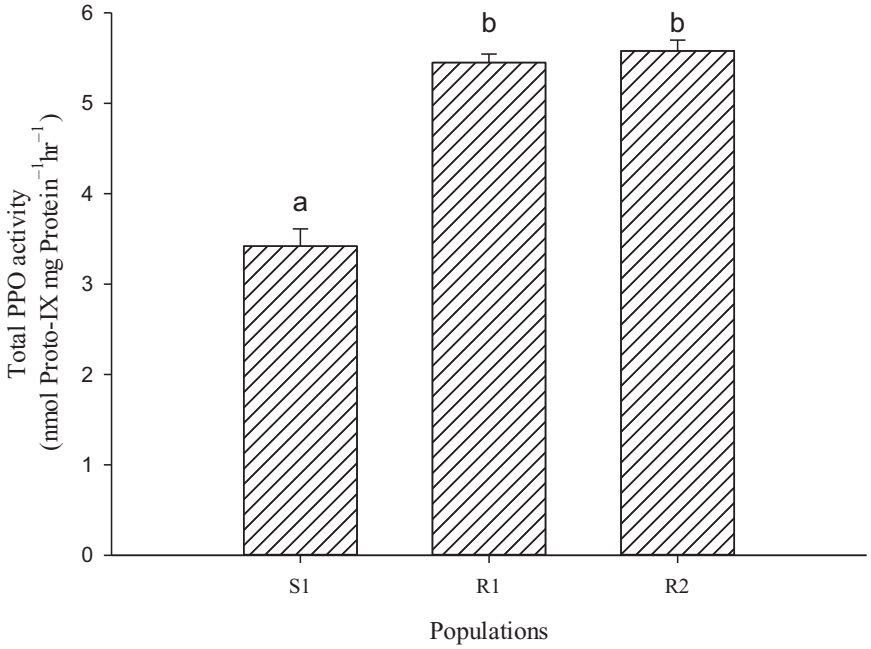

Figure 4. Extractable PPO activity in the absence of fomesafen in the resistant and susceptible *Amaranthus retroflexus* populations. Different lowercase letters indicate significant differences at the 5% level as determined by the LSD test.

https://doi.org/10.1017/wsc.2021.14 Published online by Cambridge University Press

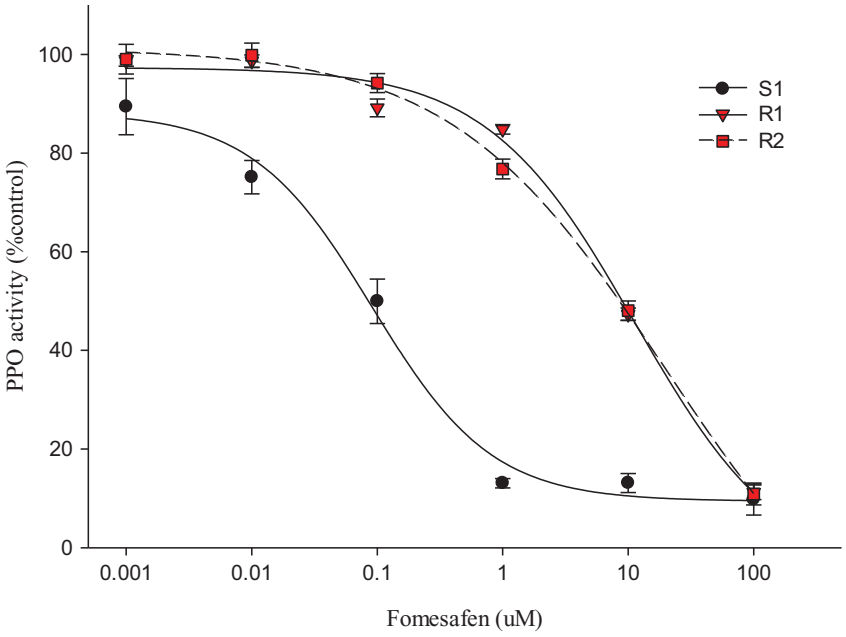

Figure 5. *In vitro* inhibition of the PPO activity of susceptible and resistant *Amaranthus retroflexus* populations by fomesafen. Mean values and their SEs are shown.

thus conferring high-level resistance to fomesafen, which might be one of the direct causes of resistance. Previous crystal structure and computational assays have revealed that Arg-128 is located in the pocket between the active site and the entryway of the substrate and that this site is crucial for stabilizing the substrate (Hao et al. 2014; Koch et al. 2004). Conformational analysis indicated that the protoporphyrinogen IX binding process should be very fast, but the protoporphyrin IX dissociation process should be slower (Hao et al. 2013). The substitution of Arg-128 with a non-polar amino acid could enlarge the mouth of the pocket, which would facilitate proto egress and thus improve the enzyme's activity. Usually, the Arg-128 mutations, including Ala-128, Ly-s128, and Glu-128, reduce the affinity between PPO and the substrate but greatly increase the catalytic speed (Hao et al. 2013; Heinemann et al. 2007).

PPO Enzyme Kinetic Analysis

The PPO K_m and V_{max} values for each population were evaluated. K_m is the substrate concentration at which the reaction rate is at half-maximum and is an inverse measure of the substrate's affinity for the enzyme. A small K_m indicates high affinity. There was no difference in PPO enzyme kinetics between the two resistant populations, but differences between the resistant and susceptible plants were significant (Table 4; Figure 5). The K_m value for the susceptible plants was 1.36 μM, and the resistant plants showed a higher K_m (approximately 2.5-fold) than the susceptible plants (Table 4). The increased K_m in the resistant plants indicates lower substrate affinity. The PPO V_{max} values for the resistant plants were 8.24 to 7.89 Proto-IX mg protein^{-1} h^{-1}, approximately 2-fold higher than those of the susceptible plants (Table 4). These results confirmed the high extractable PPO activity in the resistant plants. Although the Arg-128-Gly mutation exerted a negative impact on substrate binding, *A. retroflexus* plants containing Arg-128-Gly PPO grew normally in the absence of fomesafen. We speculate that the higher basal PPO activity in the resistant plants may have had a beneficial effect on plant growth (Figure 4). This mechanism partly explains the widespread prevalence of the Arg-128-Gly mutation. Although the enzyme still maintains its normal catalytic function, the change in enzyme conformation removes the important hydrogen-bonding interactions between enzyme and herbicide, which may lead to PPO insensitivity and, subsequently, fomesafen resistance (Hao et al. 2013, 2014). Although PPO containing Arg-128-Gly can maintain normal function, compared with that of wild-type PPO, the K_m of mutant PPO is significantly lower (Table 4). Therefore, it may exhibit obvious functional abnormalities in the case of insufficient substrate. In this regard, resistant plants containing the Arg-128-Gly mutation may reduce their fitness under certain conditions that result in a lack of substrate. However, from the actual situation, we did not observe such a fitness cost in the field or indoors. In contrast, the wide distribution of fomesafen-resistant *A. retroflexus* in soybean fields in Heilongjiang Province may imply that the Arg-128-Gly mutation may not cause a significant fitness penalty.

Table 4. Enzyme PPO K_m (μM) and V_{max} (nmol Proto-IX mg protein^{-1} h^{-1}) values of the susceptible and resistant *Amaranthus retroflexus* populations.[a]

Population	K_m	V_{max}
S1	1.36 ± 0.22	4.12 ± 0.18
R1	3.52 ± 0.49	8.24 ± 0.46
R2	3.31 ± 0.47	7.89 ± 0.44

[a]Fitting parameters and their SEs are shown.

In summary, the higher extractable PPO activity in the resistant *A. retroflexus* plants was conferred by an Arg-128-Gly substitution in *PPX2* rather than increased expression of PPO. The changes in PPO enzyme kinetics and the reduction in PPO sensitivity to fomesafen caused by the Arg-128-Gly mutation in *PPX2* are the target-site resistance mechanisms in resistant *A. retroflexus*. In addition, *PPX2* plays a more important role in resistance because of its more active expression than *PPX1* after fomesafen treatment.

https://doi.org/10.1017/wsc.2021.14 Published online by Cambridge University Press

Acknowledgments. The authors thank all workers for their assistance in conducting this research and AJE for their professional English language editing services. This work was financially supported by the National Natural Science Foundation of China (32001940), the Natural Science Foundation of Shandong Province (ZR2020QC135), the Earmarked Fund for the China Agriculture Research System (CARS-13), and the Agriculture Science and Technological Innovation Project of Shandong Academy of Agricultural Science (CXGC2018E21). The authors declare that the research was conducted in the absence of any commercial or financial relationships that could be considered as a conflict of interest.

Supplementary material. To view supplementary material for this article, please visit https://doi.org/10.1017/wsc.2021.14

References

Bradford MM (1976) A rapid and sensitive method for the quantitation of microgram quantities of protein utilizing the principle of protein-dye binding. Anal Biochem 72:248–254

Chen J, Huang Z, Zhang C, Huang H, Wei S, Chen J, Wang X (2015) Molecular basis of resistance to imazethapyr in redroot pigweed (*Amaranthus retroflexus* L.) populations from China. Pestic Biochem Physiol 124:43–47

Collavo A, Panozzo S, Lucchesi G, Scarabel L, Sattin M (2011) Characterisation and management of *Phalaris paradoxa* resistant to ACCase-inhibitors. Crop Prot 30:293–299

Dayan FE, Barker A, Tranel PJ (2018) Origins and structure of chloroplastic and mitochondrial plant protoporphyrinogen oxidases: implications for the evolution of herbicide resistance. Pest Manag Sci 74:2226–2234

Dayan FE, Daga PR, Duke SO, Lee RM, Tranel PJ, Doerksen RJ (2010) Biochemical and structural consequences of a glycine deletion in the alpha-8 helix of protoporphyrinogen oxidase. Biochim Biophys Acta 1804:1548–1556

Dayan FE, Owens DK, Tranel PJ, Preston C, Duke SO (2014) Evolution of resistance to phytoene desaturase and protoporphyrinogen oxidase inhibitors—state of knowledge. Pest Manag Sci 70:1358–1366

Deybach J-C, Silva VD, Grandchamp B, Nordmann Y (1985) The mitochondrial location of protoporphyrinogen oxidase. Eur J Biochem 149:431–435

Emanuelesson O, Nielsen H, Brunak S, Heijne G von (2000) Predicting subcellular localization of proteins based on their N-terminal amino acid sequence. J Mol Biol 300:1005–1016

Gaines TA, Zhang W, Wang D, Bukun B, Chisholm ST, Shaner DL, Nissen SJ, Patzoldt WL, Tranel PJ, Culpepper AS, Grey TL, Webster TM, Vencill WK, Sammons RD, Jiang J, *et al.* (2010) Gene amplification confers glyphosate resistance in *Amaranthus palmeri*. Proc Natl Acad Sci USA 107:1029–1034

Giacomini DA, Umphres AM, Nie H, Mueller TC, Steckel LE, Young BG, Scott RC, Tranel PJ (2017) Two new *PPX2* mutations associated with resistance to PPO-inhibiting herbicides in *Amaranthus palmeri*. Pest Manag Sci 73:1559–1563

Hao GF, Tan Y, Yang SG, Wang ZF, Zhan CG, Xi Z, Yang GF (2013) Computational and experimental insights into the mechanism of substrate recognition and feedback inhibition of protoporphyrinogen oxidase. PLoS ONE 8:e69198

Hao GF, Tan Y, Xu WF, Cao RJ, Xi Z, Yang GF (2014) Understanding resistance mechanism of protoporphyrinogen oxidase-inhibiting herbicides: insights from computational mutation scanning and site-directed mutagenesis. J Agric Food Chem 62:7209–7215

Heap I (2020) The International Survey of Herbicide Resistant Weeds. http://www.weedscience.org. Accessed: August 1, 2020

Heinemann IU, Diekmann N, Masoumi A, Koch M, Messerschmidt A, Jahn M, Jahn D (2007) Functional definition of the tobacco protoporphyrinogen IX oxidase substrate-binding site. Biochem J 402:575–580

Huang Z, Chen J, Zhang C, Huang H, Wei S, Zhou X, Chen J, Wang X (2016) Target-site basis for resistance to imazethapyr in redroot amaranth (*Amaranthus retroflexus* L.). Pestic Biochem Physiol 128:10–15

Huang Z, Cui H, Wang C, Wu T, Zhang C, Huang H, Wei S (2020) Investigation of resistance mechanism to fomesafen in *Amaranthus retroflexus* L. Pestic Biochem Physiol 165, 10.1016/j.pestbp.2020.104560

Ishida S, Miller-Sulger R, Kohno H, Böger P, Wakabayashi K (2000) Enzymatic activity of protoporphyrinogen-IX oxidase from various plant species: its sensitivity to peroxidizing herbicides. J Pest Sci 25:18–23

Jacobs JM, Jacobs NJ (1993) Porphyrin accumulation and export by isolated barley (*Hordeum vulgare*) plastids (effect of diphenyl ether herbicides). Plant Physiol 101:1181–1187

Jacobs JM, Jacobs NJ, Sherman TD, Duke SO (1991) Effect of diphenyl ether herbicides on oxidation of protoporphyrinogen to protoporphyrin in organellar and plasma membrane enriched fractions of barley. Plant Physiol 97:197–203

Koch M, Breithaupt C, Kiefersauer R, Freigang J, Huber R, Messerschmidt A (2004) Crystal structure of protoporphyrinogen IX oxidase: a key enzyme in haem and chlorophyll biosynthesis. EMBO 23:1720–1728

Lee HJ, Duke SO (1994) Protoporphyrinogen IX-oxidizing activities involved in the mode of action of peroxidizing herbicides. J Agric Food Chem 42: 2610–2618

Lee RM, Hager AG, Tranel PJ (2008) Prevalence of a novel resistance mechanism to PPO-inhibiting herbicides in waterhemp (*Amaranthus tuberculatus*). Weed Sci 56:371–375

Legleiter TR, Bradley KW, Massey RE (2009) Glyphosate-resistant waterhemp (*Amaranthus rudis*) control and economic returns with herbicide programs in soybean. Weed Technol 23:54–61

Lermontova I, Kruse E, Mock H-P, Grimm B (1997) Cloning and characterization of a plastidal and a mitochondrial isoform of tobacco protoporphyrinogen IX oxidase. Proc Natl Acad Sci USA 94:8895–8900

Nicolaus B, Sandmann G, Böger P (1993) Molecular aspects of herbicide action on protoporphyrinogen oxidase. Z Naturforsch C J Biosci 48:326–333

Nie H, Mansfield BC, Harre NT, Young JM, Steppig NR, Young BG (2019) Investigating target-site resistance mechanism to the PPO-inhibiting herbicide fomesafen in waterhemp and interspecific hybridization of *Amaranthus* species using next generation sequencing. Pest Manag Sci 75:3235–3244

Obenland O, Ma R, O'Brien S, Lygin AV, Riechers DE (2017) Resistance to carfentrazone-ethyl in tall waterhemp. Pages 30–31 *in* Proceedings of the 72nd Annual Meeting of the North Central Weed Science Society. St Louis, MO: North Central Weed Science Society of America

Odell JT, Caimi PG, Yadav NS, Mauvais CJ (1990) Comparison of increased expression of wild-type and herbicide-resistant acetolactate synthase genes in transgenic plants, and indication of posttranscriptional limitation on enzyme activity. Plant Physiol 94:1647–1654

Patzoldt WL, Hager AG, McCormick JS, Tranel PJ (2006) A codon deletion confers resistance to herbicides inhibiting protoporphyrinogen oxidase. Proc Natl Acad Sci USA 103:12329–12334

Poulson R, Polglase WJ (1975) The enzymic conversion of protoporphyrinogen IX to protoporphyrin IX. J Biol Chem 250:1269–1274

Powles SB (2010) Gene amplification delivers glyphosate-resistant weed evolution. Proc Natl Acad Sci USA 107:955–956

Powles SB, Yu Q (2010) Evolution in action: plants resistant to herbicides. Annu Rev Plant Biol 61:317–347

Rangani G, Salas-Perez RA, Aponte RA, Knapp M, Craig IR, Mietzner T, Langaro AC, Noguera MM, Porri A, Roma-Burgos N (2019) A novel single-site mutation in the catalytic domain of protoporphyrinogen oxidase IX (PPO) confers resistance to PPO-inhibiting herbicides. Front Plant Sci 10:568

Rousonelos SL, Lee RM, Moreira MS, Vangessel MJ, Tranel PJ (2012) Characterization of a common ragweed (*Ambrosia artemisiifolia*) population resistant to ALS- and PPO-inhibiting herbicides. Weed Sci 60:335–344

Salas RA, Burgos NR, Tranel PJ, Singh S, Glasgow L, Scott RC, Nichols RL (2016) Resistance to PPO-inhibiting herbicide in Palmer amaranth from Arkansas. Pest Manag Sci 72:864–869

Seefeld SS, Jensen JE, Fuerst EP (1995) Log-logistic analysis of herbicide dose-response relationships. Weed Technol 9:218–227

Shoup DE, Al-Khatib K, Peterson DE (2003) Common waterhemp (*Amaranthus rudis*) resistance to protoporphyrinogen oxidase-inhibiting herbicides. Weed Sci 51:145–150

Tranel PJ (2002) Resistance of weeds to ALS-inhibiting herbicides: what have we learned. Weed Sci 50:700–712

Trezzi M, Felippi C, Mattei D, Silva H, Nunes A, Debastiani C, Vidal R, Marques A (2005) Multiple resistance of acetolactate synthase and protoporphyrinogen oxidase inhibitors in *Euphorbia heterophylla* biotypes. J Environ Sci Health B 40:101–109

Varanasi VK, Brabham C, Korres NE, Norsworthy JK (2019) Nontarget site resistance in Palmer amaranth [*Amaranthus palmeri* (S.) Wats.] confers cross-resistance to protoporphyrinogen oxidase-inhibiting herbicides. Weed Technol 33:349–354

Varanasi VK, Brabham C, Norsworthy JK (2018a) Confirmation and characterization of non–target site resistance to fomesafen in Palmer amaranth (*Amaranthus palmeri*). Weed Sci 66:702–709

Varanasi VK, Brabham C, Norsworthy JK, Nie H, Young BG, Houston M, Barber T, Scott RC (2018b) A Statewide survey of PPO-inhibitor resistance and the prevalent target-site mechanisms in palmer amaranth (*Amaranthus palmeri*) accessions from Arkansas. Weed Sci 66:149–158

Wang H, Guo W, Zhang L, Zhao K, Ge L, Lv X, Liu W, Wang J (2017) Multiple resistance to thifensulfuron-methyl and fomesafen in redroot pigweed (*Amaranthus retroflexus* L.) from China. Chilean J Agric Res 77:311–317

Wang H, Wang H, Zhao N, Zhu B, Sun P, Liu W, Wang J (2019) Multiple resistance to PPO and ALS inhibitors in redroot pigweed (*Amaranthus retroflexus*). Weed Sci 68:1–8

Watanabe N, Che FS, Iwano M, Takayama S, Yoshida S, Isogai A (2001) Dual targeting of spinach protoporphyrinogen oxidase II to mitochondria and chloroplasts by alternative use of two in-frame initiation codons. J Biol Chem 276:20474–20481

Yang S, Hao G, Dayan FE, Tranel PJ, Yang G (2013) Insight into the structural requirements of protoporphyrinogen oxidaseinhibitors: molecular docking and CoMFA of diphenyl ether, isoxazole phenyl, and pyrazole phenyl ether. Chin J Chem 31:1153–1158

Young BG (2006) Changes in herbicide use patterns and production practices resulting from glyphosate-resistant crops. Weed Technol 20:301–307

https://doi.org/10.1017/wsc.2021.14 Published online by Cambridge University Press